Structural and magnetic behavior of Fe(Nb,Zr) rich alloys produced by mechanical alloying

Cite as: AIP Advances **8**, 047704 (2018); https://doi.org/10.1063/1.4994144
Submitted: 04 July 2017 . Accepted: 07 August 2017 . Published Online: 12 October 2017

A. Carrillo, L. Escoda, J. Saurina, and J. J. Suñol

Structural and magnetic behavior of Fe(Nb,Zr) rich alloys produced by mechanical alloying

A. Carrillo, L. Escoda, J. Saurina, and J. J. Suñol[a]
EPS, C/Univesritat de Girona 4, University of Girona, 17003 Girona, Spain

(Received 4 July 2017; accepted 7 August 2017; published online 12 October 2017)

$Fe_{80}Nb_7B_{12}Cu_1$ and $Fe_{80}(NiZr)_7B_{12}Cu_1$, nanocrystalline alloys were synthesized in two high-energy ball milling devices (planetary, shaker). The microstructure, thermal and magnetic properties of the milled powders were characterized by X-ray diffraction (XRD), differential scanning calorimetry (DSC) and vibrating sample magnetometry (VSM); respectively. Milling device influences the microstructure and properties of final products. The results suggest more energetic milling in shaker mill. The main phase is always bcc Fe rich solid solution. Nevertheless, in $Fe_{80}Nb_7B_{12}Cu_1$ alloy minor Nb(B) phase is found after shaker milling and in $Fe_{80}(NiZr)_7B_{12}Cu_1$ alloy a low crystalline size Zr rich phase after planetary milling. Crystalline grain size ranges between 9.5 and 15.1 nm; lower values correspond to alloys with a second minor phase. Coercivity values ranges between 28.6 and 36.9 Oe.
https://doi.org/10.1063/1.4994144

INTRODUCTION

Fe-M-B alloys with M an early transition metal (so called Nanoperm) are known to be usually soft-magnetic materials due their high saturation magnetization, good permeability and low magnetocrystalline anisotropy, Makino *et al.* (1997). These alloys are generally obtained as amorphous by rapid solidification techniques and nanocrystalline structure was found after an ulterior annealing, Skorvanek *et al.* (1999). On the other hand, these compositions can be also obtained directly as nanocrystalline grains by mechanical alloying (MA), Blázquez *et al.* (2014). MA is a solid-state powder processing technique that can produce a variety of equilibrium and non-equilibrium alloy phases at a nanoscale level, Suñol *et al.* (2004). During MA of Fe rich alloys, an important fraction of grains boundaries is created leading, generally, to the apparition of novel physical properties, especially, magnetic ones. Likewise, in the last decades, many researchers have been carried out experimental studies to investigate the alloying effect of systems with three, four or even more elements, Miglierini *et al.* (2016), Hocine *et al.* (2017), Kong *et al.* (2011). One option is the addition of a minor amount of copper as in Finemet alloys. In this work we analyze the nanostructure, thermal stability and magnetic response of two Fe(Nb,Zr) rich alloys produced by mechanical alloying. The competition during alloying between different elements sometimes is not well understand and therefore needs more carefully investigations. Furthermore, alloying is also influenced by milling processing parameters and devices. For it, milling was performed in two milling devices for 80 hours to detect their influence on milled nanostructured samples.

EXPERIMENTAL

Mechanical alloying was carried out in two high-energy ball milling devices: a) planetary ball mill (Fritsch Pulverisette P7) and b) shaker mill (SPEX 8000). Milling was performed starting from

[a]corresponding author: joanjosep.sunyol@udg.edu

pure element and compound powders. Fe of 99.7% purity, with a particle size under 8 μm; Nb of 99.85% purity, with a particle size under 74 μm; Cu 99.8% purity, particle size under 45 μm, B of 99.6% purity, with a particle size 50 μm; and prealloyed $Ni_{70}Zr_{30}$ powders (purity of 99.9% and particle size >150 μm).

The nominal compositions produced and analyzed were $Fe_{80}Nb_7B_{12}Cu_1$ and $Fe_{80}(NiZr)_7B_{12}Cu_1$, labeled as A and B, respectively. In both devices, milling was performed during 80h in CrNi steel vials and the powder to balls mass ratio was fixed at 1:5. The containers were sealed in a glove box with a stationary argon atmosphere. The MA powders were thermally characterized by differential scanning calorimetry (DSC) in DSC30 Mettler-Toledo equipment. X-ray diffraction (XRD) structural analysis was carried out using D-500 Siemens equipment using Cu K_α radiation. Magnetic measurements were performed by vibrating sample magnetometry (VMS) in a Lake-Shore device.

RESULTS AND DISCUSSION

The formation of the nanocrystalline structure by mechanical alloying was checked by X-ray diffraction. Figure 1 show the XRD patterns corresponding to the alloy A after 80 h milling. In alloy milled with SPEX only bcc-Fe rich solid solution phase was found. This phase is the main phase

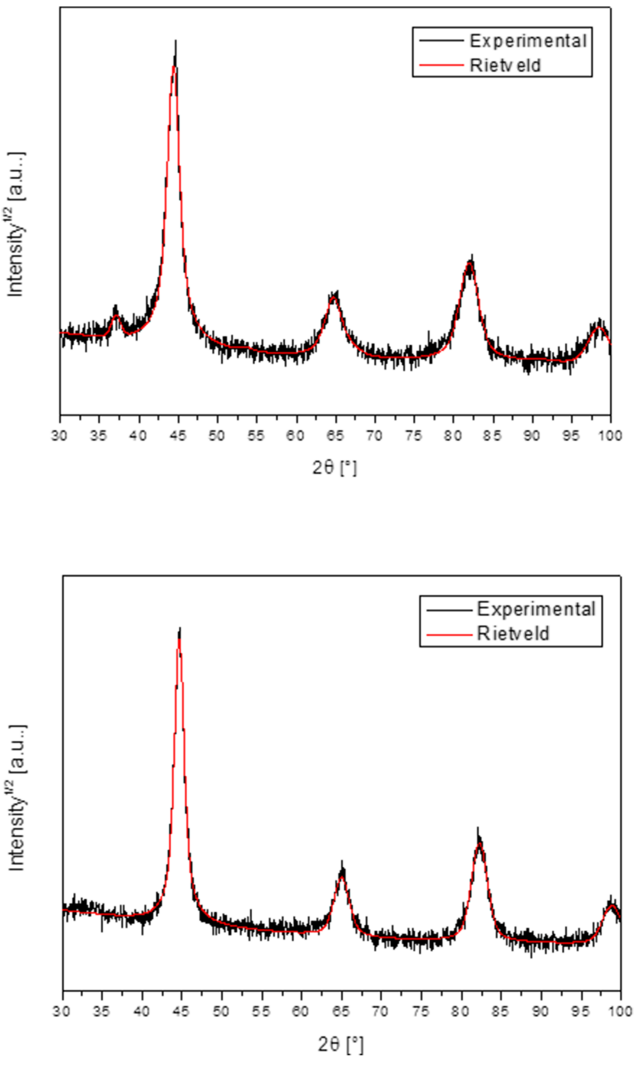

FIG. 1. XRD patterns of FeNbBCu alloy after 80h of milling. Up (P7), down (SPEX).

in alloy milled in P7 device. Likewise, in this sample, a minor phase associated to Nb(B) rich solid solution is also found. In alloys with Fe and B milling sometimes favors the apparition of Fe-B compounds, but in Nb-B milling the Nb(B) rich phase here detected was also found in the literature, Izumi *et al.*, 2006. The reaction between B and Nb is related to the negative enthalpy of mixing: ~ -39 kJ/mol. This fact indicates that milling with SPEX allows to the formation of a unique phase whereas probably additional milling time is needed in P7 device, as it was obtained in Fe-Nb-B milled alloys by Alleg *et al.*, 2010. This seems indicate a higher milling intensity and energy transfer to the sample in SPEX device.

Figure 2 show the XRD patterns corresponding to the nanocrystalline alloy B obtained after 80 h milling. In this alloy, the bcc Fe based phase was also found. The main difference is that Zr rich nanocrystalline solid solution was found in sample milled with SPEX. This Zr phase was previously found in other FeZr based alloys, Pilar *et al.* (2008). In the FeNiZrBCu alloy, P7 milling is more effective to obtain a single nanocrystalline phase and milling in SPEX device produces the formation of a Zr phase coexisting with the nanocystalline main phase. Nb and Zr atoms have high atomic radius and this fact does not favor its introduction in the solid solution, Pilar *et al.* (2007).

The microstructural and structural parameters were obtained, from the Rietveld refinement of the XRD patterns, by applying the MAUD Program, Lutterotti *et al.* (1999). Results of the main bcc-Fe rich phase are given in Table I. The lattice parameter is always higher that 0.2856 nm

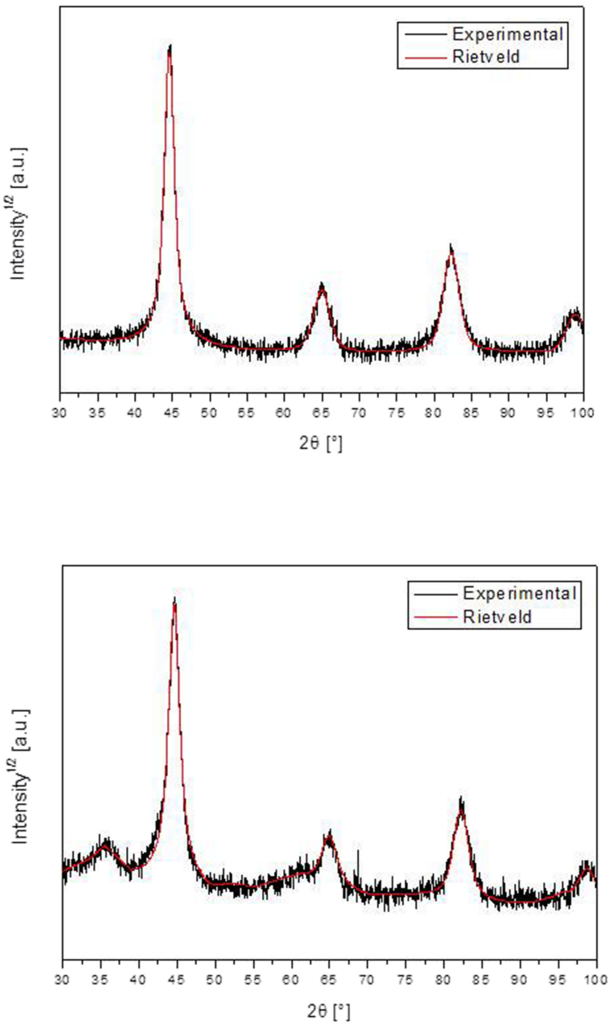

FIG. 2. XRD patterns of FeNiZrBCu alloy after 80h of milling. Up (P7), down (SPEX).

TABLE I. Lattice constant, a, crystalline size, L, microstrain, ε, and density of dislocations, ρ.

Sample	a (nm)	L (nm)	ε (%)	ρ (10^{15} m^{-2})
A (P7)	0.28832(3)	9.9(4)	0.66(5)	9.1(7)
A (SPEX)	0.28694(2)	15.1(9)	0.6(1)	5.5(9)
B (P7)	0.28706(2)	13.4(5)	0.59(6)	6.2(6)
B (SPEX)	0.28717(3)	9.5(2)	0.40(3)	5.9(4)

(pure bcc Fe) indicating the formation of a solid solution. All alloys are nanocrystalline (crystalline size range between 9.5 and 15.1 nm). Lower values were found in samples with a minor phase. Thus, as increasing the content of Nb and Zr atoms inside the solid solution, a higher grain size was achieved. Microstrain values ranged between 0.40(3) and 0.66(5), values similar to those found in the literature for Fe rich ball milled alloys, Alleg *et al.* (2013). Furthermore, the density of dislocations has been also calculated taking into account the expression given by Williamson and Smallman *et al.* (1956). The values are slightly lower than dislocation density limit in metal achieved by plastic deformation ($10^{16}/m^2$ for edge dislocations), Eckert *et al.* (1992).

The general character of the DSC traces for all samples is similar. Figure 3 show the results corresponding to alloy A milled for 80 h. The exothermic process at ~200 K is due to structural relaxation of milled alloy. The broad exothermic process starting at ~250–300 K might be due to early surface crystallization (particle surface) coupled with internal stress, Ipus *et al.* (2013). The main crystallization process (detected in alloy milled in SPEX at ~ 500 K) is related to the crystalline growth of the bcc Fe phase. Figure 4 show DSC scans of alloy B. The broad exothermic processes detected by DSC correspond to different Fe environments probable favored by Ni addition in alloy B, Suñol *et al.* (2007). In sample milled in P7 device the small exothermic peak at ~350 K is linked to crystalline growth of the bcc Fe rich phase. Likewise, in alloy B milled in SPEX a very intense crystallization peak (~550 K) is found. As higher is the temperature of the crystalline growth exothermic peak, higher is the thermal stability of the nanocrystalline alloy front crystallization. The behavior here found is different than crystallization from amorphous phase. The crystallization of as-quenched amorphous ribbons is reported by Makino *et al.* (1994) in Fe–X–B (X = Zr, Hf or Nb) alloys. The amorphous phase crystallizes in a two-stage crystallization process in which a single bcc Fe nanocrystalline phase appears after the first stage, and coarse bcc Fe grains with intermetallic phases appear after the second stage. The reported temperature of the second crystallization stage (>1000 K) is higher than the maximum temperature achieved in our DSC equipment.

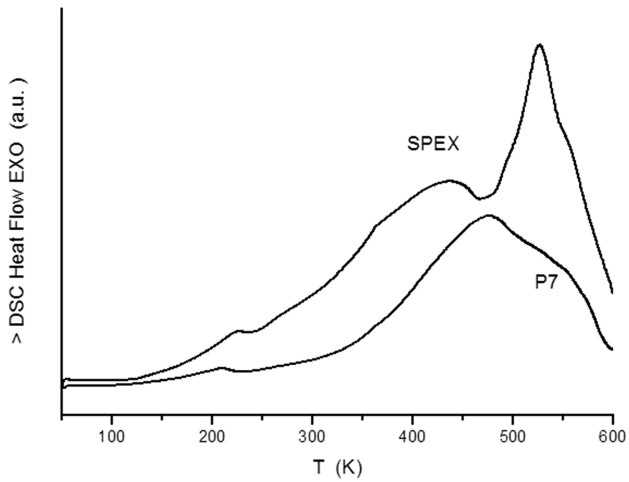

FIG. 3. DSC scans of FeNbBCu alloy after 80h of milling.

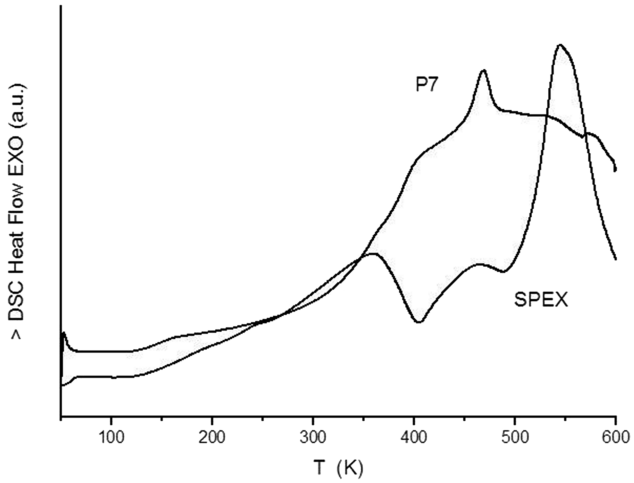

FIG. 4. DSC scans of FeNiZrBCu alloy after 80h of milling.

Magnetic hysteresis cycles, at room temperature, were shown in figures 5 and 6 corresponding to alloys A and B, respectively. Such sigmoidal hysteresis cycles are usually observed in nanostructured samples with small magnetic domains. This is due not only to the presence of structural distortions inside grains, but also to a higher density of nanocrystalls which hinder the domain wall motion. Results are given in Table II. All the studied samples present in the nanocrystalline state ferromagnetism at room temperature and have low coercivity, H_c, values (ranged between 28.6 and 36.9 Oe) which are the most important requirements for a soft magnetic material. Coercivity values are similar to those found in literature, Ipus *et al.* (2013). Lower coercivity was found in the two samples with only one crystalline phase (higher difference in alloy B). Thus, second phase is not as soft magnetic than Fe rich bcc main phase and provokes an increase of H_c, There are other considerations to be take into account. As regarding boron element influence, sometimes boron inclusions were formed; Ipus *et al.* (2009). These inclusions can be not detected by XRD favoring the hardening of the alloy. Likewise, an amount of niobium/zirconium can remain in the grain boundaries.

The decrease of the saturation magnetization, M_s, was measured in alloy A milled in SPEX. This decrease usually suggests remarkable change of the magnetic moment during the alloying due to the change of the nearest neighbor configuration of the magnetic element, Fe. This effect is coherent with the existence of non-magnetic niobium and boron atoms in the vicinity of iron sites reducing the

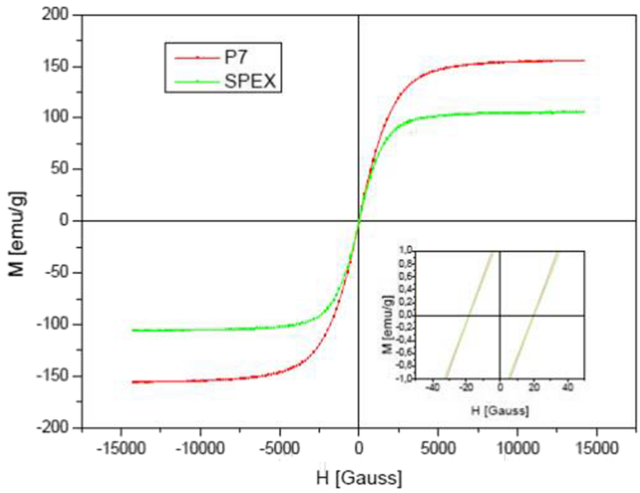

FIG. 5. Hysteresis loops at room temperature of FeNbBCu alloy after 80h of milling.

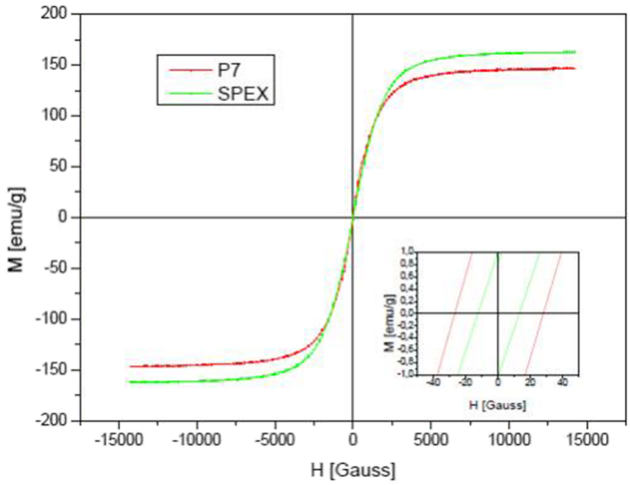

FIG. 6. Hysteresis loops at room temperature of FeNiZrBCu alloy after 80h of milling.

TABLE II. Coercivity, H_c, and magnetization of saturation, M_s.

Sample	H_c (Oe)	M_s (emu/g)
A (P7)	30.7(4)	155.6
A (SPEX)	29.2(4)	105.3
B (P7)	28.6(4)	146.1
B (SPEX)	36.9(5)	162.6

magnetic moment, Alleg *et al.* (2013). In alloy A milled in P7 a big amount of minor elements are in Nb(B) phase detected by XRD. Minor differences were found in alloy B. Slight diminution in the magnetization of saturation is due to highly disordered Zr rich phase. It is known that the saturation of magnetization increases as increasing crystalline fraction, Ipus *et al.* (2013). Thus, milling device influences soft magnetic behavior of the final product.

Furthermore, usually MA samples have always higher coercivity values than samples prepared by other routes, for example melt-spinning, Tsepelev *et al.*, 2017. Nevertheless, these nanocrystalline materials (ribbon shape) have limited applications due to restriction on core winding process, Shyni *et al.* (2015). In MA alloys the decrease of the grain size to the nanoscale favors soft magnetic behavior. Nevertheless, MA provokes the increase of microstrain and, therefore, of coercivity. One option to reduce microstrain and coercivity is the annealing of the milled powders. It is necessary the optimization of the annealing process to reduce microstrain level (and coercivity) without a significant increase of crystalline size (and preventing the formation of undesired phases).The main problem is that coercivity values lower than 100 KA/m are not achieved. One option is the ball milling of ribbons, Torrens-Serra *et al.*, 2009.

CONCLUSIONS

Two nanocrystalline $Fe_{80}Nb_7B_{12}Cu_1$ (A) and $Fe_{80}(NiZr)_7B_{12}Cu_1$ (B) nanocrystalline alloys were synthesized in two (planetary, shaker) high-energy ball milling devices. Nanocrystalline size ranged between 9.5 and 15.1 nm. Lower crystalline size was found in samples with a second minor phase. Milling on shaker mill favors the formation of a unique phase in alloy A, and the formation of minor Zr rich solid solution in alloy B. All samples are soft magnetic at room temperature. Lower coercivity values (28.6 and 29.2 Oe) were found in the two samples with only one crystalline phase. Thus, in soft ferromagnetic alloys produced by mechanical alloying, final product microstructure and the material properties depends of milling device. Results seem indicate that shaker mill is more energetic.

ACKNOWLEDGMENTS

Financial support from Spanish MINECO under project MAT2016-75967-P is gratefully acknowledged.

Alleg, S., Hamouda, A., Azzaza, S., Bensalem, R., Suñol, J. J., and Greneche, J. M., "Solid state amorphization transformation in the mechanically alloyed $Fe_{28.9}Nb_{2.2}B_{69.9}$ powders," Materials Chemistry and Phyics **122**, 35–40 (2010).

Alleg, S., Kartout, S., Ibrir, M., Azzaza, S., Fenineche, N. E., and Suñol, J. J., "Magnetic, structural and thermal properties of the finemet-type powders prepared by mechanical alloying," Journal of Physics and Chemistry of Solids **74**, 550–557 (2013).

Blázquez, J. S., Ipus, J. J., Conde, C. F., and Conde, A., "Evolution of Fe environments in mechanically alloyed Fe-Nb-(B) compositions," Journal of Alloys and Compounds **615**, S555–S558 (2014).

Eckert, J., Holzer, J. C., Krill, C. E., and Johnson, W. L., "Structural and thermodynamic properties of nanocrystalline fcc metals prepared by mechanical attrition," Journal of Materials Research **7**, 1751–1761 (1992).

Hocine, M., Guittoum, A., Hemmous, M., Martínez-Blanco, D., Gorria, P., Rahal, B., Blanco, J. A., Suñol, J. J., and Laggoun, A., "The role of silicon on the microstructure and magnetic behavior of nanostructured (Fe0.7Co0.3)100-xSix powders," Journal of Magnetism and Magnetic Materials **422**, 149–156 (2017).

Ipus, J. J., Blázquez, J. S., Lozano-Pérez, S., and Conde, A., "Microstrutural evolution characterization of Fe-Nb-B ternary systems processed by ball milling," Philosophical Magazine **89**(17), 1415–1423 (2009).

Ipus, J. J., Blázquez, J. S., Franco, V., and Conde, A., "The use of amorphous boron powder enhances mechanical alloying in soft magnetic FeNbB alloy: A magnetic study," Journal of Applied Physics **113**, 17A330 (2013).

Izumi, K., Sekiya, C., Okada, S., Kudou, K., and Shishido, T., "Mechanochemically alloyed assisted preparation of NbB_2 powder," Journal of the European Ceramic Society **26**, 635–638 (2006).

Kong, L. H., Gao, Y. L., Song, T. T., and Zhai, Q. J., "Structure and magnetic properties of Nb doped FeZrB soft magnetic alloys," Journal of Magnetism and Magnetic Materials **323**, 2165–2169 (2011).

Lutterotti, L., Matthies, S., and Wenk, H. R., "MAUD: A friendly Java program for material analysis using diffraction," IUCr: Newsletter of the CPD (1999).

Makino, A., Suzuki, K., Inoue, A., and Masumoto, T., "Magnetic properties and core losses of nanocrystalline Fe-M-B (M = Zr, Hf or Nb) alloys," Materials Science and Engineering A **179**, 127–131 (1994).

Makino, A., Hatanai, T., Inoue, A., and Masumoto, T., "Nanocrystalline soft magnetic Fe-M-B (M=Zr, Hf, Nb) alloys and their applications," Materials Science and Engineering A **226**, 594–602 (1997).

Miglierini, M. and Hasiak, M., "Ion irradiation induced structural modifications of Fe81Mo8Cu1B10 nanoperm-type alloy," Physica Sttus Solidi A – Applications and Materials Science **213**, 1138–1144 (2016).

Pilar, M., Suñol, J. J., Bonastre, J., and Escoda, L., "Influence of process control agents in the development of a metastable Fe-Zr based alloy," Journal of Non-Crystalline Solids **353**, 848–850 (2007).

Pilar, M., Escoda, L., Suñol, J. J., and Greneche, J. M., "Magnetic study and thermal analysis of a metastable Fe-Zr based alloy: Influence of process control agents," Journal of Magnetism and Magnetic Materials **320**, e123–e127 (2008).

Skorvanek, I., Kovac, J., Marcin, J., Duhaj, P., and Gerling, R., "Annealing effects on the magnetic properties of nanocrystalline FeNbB alloys," Journal of Magnetism and Magnetic Materials **203**, 226–228 (1999).

Shyni, P. C. and Perumal, A., "Structural and magnetic properties of nanocrystalline Fe-Co-Si alloy poders by mechanical alloying," Journal of Alloys and Compounds **648**, 658–666 (2015).

Suñol, J. J., González, A., Saurina, L., Escoda, L., and Bruna, P., "Thermal and structural characterization of Fe-Nb-B alloys prepared by mechanical alloying," Naterials Science and Engineering A **375-377**, 874–880 (2004).

Suñol, J. J., González, A., Saurina, J., Escoda, L., and Fernández-Barquín, L., "Thermal and magnetic behavior of a nanocrystalline Fe(Ni,Co) based alloy," Journal of Non-Crystalline Solids **353**, 865–868 (2007).

Torrens-Serra, J., Bruna, P., Roth, S., Rodríguez-Viejo, J., and Clavaguera-Mora, M. T., "Bulk soft magnetic materials from ball milled $Fe_{77}Nb_7B_{15}Cu_1$ amorphous ribbons," Intermetallics **17**, 79–85 (2009).

Tsepelev, V., Starodubtsev, Y., Konashkov, V., and Belozerov, V., "Thermomagnetic analysis of soft magnetic nanocrystalline alloys," Journal of Alloys and Compounds **707**, 210–213 (2017).

Williamson, G. K. and Smallman, R. E., "Dislocation density in some annealed and cold-worked metals from measurements on the X-ray Debye-Scherrer spectrum," Philosophical Magazine **1**, 34–46 (1956).